LUND UNIVERSITY

Sum rules for lossless antennas

Gustafsson, Mats

Published in:
IET Microwaves, Antennas and Propagation

DOI:
10.1049/iet-map.2009.0083

2010

Document Version:
Peer reviewed version (aka post-print)

Link to publication

Citation for published version (APA):
Gustafsson, M. (2010). Sum rules for lossless antennas. *IET Microwaves, Antennas and Propagation*, *4*(4), 501-511. https://doi.org/10.1049/iet-map.2009.0083

Total number of authors:
1

General rights
Unless other specific re-use rights are stated the following general rights apply:
Copyright and moral rights for the publications made accessible in the public portal are retained by the authors and/or other copyright owners and it is a condition of accessing publications that users recognise and abide by the legal requirements associated with these rights.
• Users may download and print one copy of any publication from the public portal for the purpose of private study or research.
• You may not further distribute the material or use it for any profit-making activity or commercial gain
• You may freely distribute the URL identifying the publication in the public portal

Read more about Creative commons licenses: https://creativecommons.org/licenses/

Take down policy
If you believe that this document breaches copyright please contact us providing details, and we will remove access to the work immediately and investigate your claim.

LUND UNIVERSITY

PO Box 117
221 00 Lund
+46 46-222 00 00

Download date: 04. May. 2026

Sum rules for lossless antennas

Mats Gustafsson

***Abstract*—In this paper, sum rules for the antenna input impedance and admittance are introduced. These identities relate the radiation resistance and conductance integrated over all frequencies with the low-frequency capacitance and inductance. They are valid for lossless antennas and particularly useful for small antennas that utilize their first resonance. Numerical results for various antennas are used to illustrate the sum rules.**

I. Introduction

The antenna input impedance is a function of frequency. Its particular dynamical behavior is governed by the Maxwell equations and is determined experimentally or numerically. In this paper, it is shown that some weighted integrals of the input impedance are related to the low-frequency capacitance and inductance of the antenna. These type of relations are often referred to as sum rules and they are important for physical understanding as well as deriving physical bounds on various systems [1], [2]. In antenna theory, they offer a generalization the classical physical bounds on antennas by Chu [3] to circumscribing geometries of arbitrary shape [4], [5], [6], [7]. Sum rules are also of great importance in quantum mechanics [2], matching theory [8], scattering theory [9], meta materials [10], [11], extra ordinary transmission [12], and for radar absorbers [13].

The derivation of the sum rules in this paper are based on the assumptions of linearity, time-translational invariance, continuity, causality, and passivity. Linearity together with continuity and time-translational invariance offer a representation of the system in the form of a temporal convolution [14], [15]. This is also the basic requirement for time harmonic analysis as the convolution operator is diagonalized by the Laplace transform, *cf.*, the impulse response and transfer function in system theory [16], [14], [15]. Causality restricts the convolution kernel to be zero for negative times, which corresponds to analyticity in the Laplace domain, *i.e.*, for complex-valued frequencies. Finally, passivity adds a positive sign on the real-valued part in the Laplace domain and extends its definition up to the imaginary axis, *i.e.*, for $\operatorname{Re} s > 0$, $Z(s)$ is holomorphic and $\operatorname{Re} Z(s) \geq 0$, where Z denotes the impedance of the system. These functions are the positive real functions [17], [15] and the sum rules follow from mathematical identities that relate weighted integrals of $\operatorname{Re} Z$ with the low- and high-frequency asymptotes of Z [16].

It should be noted that the considered assumptions above are related and it can be shown that passivity imply causality in many cases [14]. It is also observed that it is common to use the upper [18] instead of the right complex half plane in *e.g.*, mathematics and theoretical physics, where the corresponding function class is called Herglotz or Nevanlinna functions [16], [2].

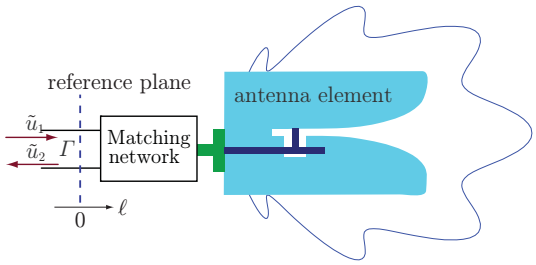

Fig. 1. Illustration of an antenna connected to a matching network and a transmission line.

In this paper, it is shown that the input impedance, input admittance, and the logarithm of the reflection coefficient generate positive real functions for linear antennas [19]. Associated sum rules for reciprocal and lossless antennas are derived using Cauchy integrals under basic assumptions on the low- and high-frequency asymptotes. The sum rules relate the radiation resistance and conductance integrated over all frequencies with the low-frequency inductance, L, and capacitance, C. It is also shown that L and C can be used to estimate the bandwidth for simple antennas that act as an open circuit in the low-frequency limit and has a dominating first resonance.

This paper is organized as follows. In Sec. II, low- and high-frequency properties of the reflection coefficient are presented and used to obtain bounds on the bandwidth. The input impedance and admittance for antennas that act as open and short circuits in the static limit are analyzed in Secs III and IV, respectively. Relations with the Chu bound are demonstrated in Sec. V. Numerical illustrations are presented in Secs VI and VII.

II. The reflection coefficient of single port antennas

Consider an arbitrary single port antenna system that is connected to a transmission line with characteristic impedance Z_0, see Fig. 1. As the derivation is solely based on linearity, continuity, time-translational invariance, causality, and passivity there are no additional complications to include a passive matching network [8] in the antenna system. The matching network is modeled by combinations of lumped circuit elements and microwave components. The total system is assumed to be linear and lossless, *i.e.*, it is composed of linear and lossless materials. It is also assumed that Z_0 is frequency independent and that there is a single propagating mode on the transmission line for low frequencies.

Let an incident signal $\tilde{u}_1(t-\ell/c)$ propagate on the transmission line (lowest order mode) with speed c towards the antenna, where ℓ denotes the distance from the reference plane,

see Fig. 1. The mismatch due to the transmission line and antenna interface creates a reflected signal $\tilde{u}_2(t+\ell/c)$ that due to linearity, time-translational invariance, continuity, and causality can be expressed as

$$\tilde{u}_2(t) = \int_{0-}^{\infty} \Gamma_{\rm t}(t')\tilde{u}_1(t-t')\,{\rm d}t', \tag{1}$$

where $\Gamma_{\rm t}$ denotes the convolution kernel of the reflection operator [14], [15] and $0-$ is the limit $0 < \delta \to 0$ that is essential for instantaneously reflected signals. The Laplace transform of (1) simplifies the relation to $u_2(s) = \Gamma(s)u_1(s)$ where

$$\Gamma(s) = \int_{0-}^{\infty} {\rm e}^{-st}\Gamma_{\rm t}(t)\,{\rm d}t \tag{2}$$

is the reflection coefficient, $s = \sigma + {\rm j}\omega$ denotes the Laplace parameter with $\sigma \geq 0$, ${\rm j}^2 = -1$, and ω is the angular frequency. Note that several modes propagate on a transmission line for high frequencies. Hence, it is useful to introduce a scattering matrix to model the transmission line and antenna interface [20] and to identify the reflection coefficient, Γ, with the diagonal element of the lowest order mode that dominates the wave propagation for low frequencies.

Based on the assumption of an asymptotic expansion of the reflection coefficient Γ and application of passivity and scattering theory, see Appendix A, it is shown that $\Gamma(s)$ is holomorphic, bounded $|\Gamma(s)| \leq 1$, and symmetric $\Gamma(s) = \Gamma(s^*)^*$ in ${\rm Re}\, s > 0$ and has the expansion

$$\pm\Gamma(s) = 1 - \nu_1 s + \nu_1^2 s^2/2 + \nu_3 s^3 + \mathcal{O}(s^4) \quad \text{as } s \to 0, \tag{3}$$

where $\nu_1 > 0$. The two cases $\Gamma(0) = 1$ and $\Gamma(0) = -1$ model antennas that act as open and short circuits in the static limit, respectively.

As the reflection coefficient is bounded in magnitude by unity, conformal maps of the unit circle to the right complex half plane produce positive real functions [17]. In this paper, two transforms are specially examined, first the logarithm $-\ln\Gamma$ and secondly the Cayley transform $(1+\Gamma)/(1-\Gamma)$. The second case generates sum rules for the impedance and the admittance, see Secs III and IV. The first case with the logarithm of the reflection coefficient resemble the Fano approach to broad-band matching [8], and it is analyzed below.

From (3) it is given that the logarithm of Γ has the low-frequency expansion

$$-\ln\big(\pm\Gamma(s)\big) = \nu_1 s - (\nu_3 + \nu_1^3/6)s^3 + \mathcal{O}(s^4) \quad \text{as } s \to 0. \tag{4}$$

The corresponding high-frequency asymptote is at most linear, *i.e.*,

$$-\ln\big(\pm\Gamma(s)\big) = \nu_\infty s + o(s) \quad \text{as } s \to \infty, \tag{5}$$

where $\nu_\infty \geq 0$. The linear term models a time delay and it can always be set to zero by translation of the reference plane towards the antenna, see Fig. 1.

Since Γ may have zeros in the right complex half plane it is necessary to remove these. Construct the Blaschke product [2] $\prod_{m=1}^{\infty}(s_m - s)/(s_m^* + s)$ where s_m, $m = 1, 2, \ldots$ denote the zeros of Γ in ${\rm Re}\, s > 0$, and define the positive real function

$$h(s) = -\ln\left(\Gamma(s)\prod_{m=1}^{\infty}\frac{s_m^* + s}{s_m - s}\right). \tag{6}$$

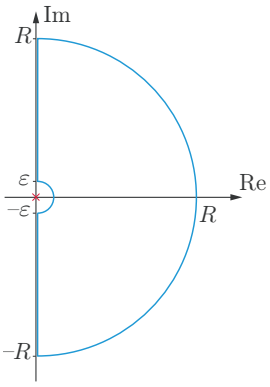

Fig. 2. The integration contour for the Cauchy integral with $\varepsilon \to 0$ and $R \to \infty$.

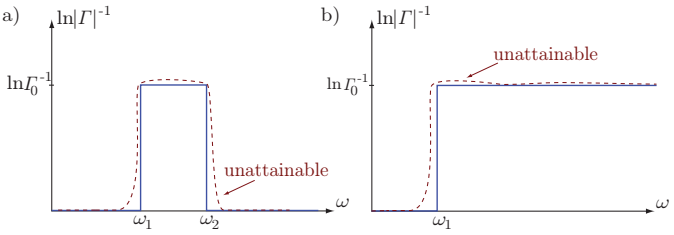

Fig. 3. Illustrations of the physical bounds. The weighted areas under the solid curves are bounded by the low-frequency properties of Γ. The dashed curves illustrate unattainable reflection coefficients. a) fractional bandwidth with $\omega \in [\omega_1, \omega_2]$. b) ultra wideband (UWB) with $\omega \in [\omega_1, \infty]$.

It is holomorphic in ${\rm Re}\, s > 0$ where ${\rm Re}\, h(s) \geq 0$ and ${\rm Re}\, h$ is independent of the Blaschke product at the frequency axis, *i.e.*, ${\rm Re}\, h({\rm j}\omega) = -\ln|\Gamma({\rm j}\omega)| \geq 0$.

The expansion (4) shows that it is possible to derive two integral identities, *cf.*, App. A and [8]. Integrate $h(s)/s^2$ and $h(s)/s^4$ over the contour depicted in Fig. 2 to get the following integral identities:

$$\frac{2}{\pi}\int_0^{\infty}\frac{1}{\omega^2}\ln\frac{1}{|\Gamma({\rm j}\omega)|}\,{\rm d}\omega = \nu_1 - \nu_\infty - 2\sum_m {\rm Re}\,\frac{1}{s_m} \tag{7}$$

and

$$\frac{2}{\pi}\int_0^{\infty}\frac{1}{\omega^4}\ln\frac{1}{|\Gamma({\rm j}\omega)|}\,{\rm d}\omega = \nu_3 + \nu_1^3/6 + \frac{2}{3}\sum_m {\rm Re}\,\frac{1}{s_m^3}. \tag{8}$$

Note that the results in (7) and (8) are independent of the location of the reference plane, see Fig. 1. A translation of the reference plane at $\ell = 0$ to $\ell = \ell_1$ transforms the reflection coefficient as $\Gamma_{\ell_1}(s) = {\rm e}^{-2\ell_1 s/{\rm c}_0}\Gamma_0(s)$ and hence $-\ln\Gamma_{\ell_1}(s) = 2\ell_1 s/{\rm c}_0 - \ln\Gamma_0(s)$, where it is observed that $2\ell_1 s/{\rm c}_0$ is added to both the low- and high-frequency asymptotes. Below, it assumed that the reference plane is placed such that $\nu_\infty = 0$.

The integral identities (7) and (8) are used to derive bounds on the reflection coefficient and bandwidth, *cf.*, the Fano bound for lossless matching networks [8], [21], Fig. 3, and App. A. The narrowband result, $B \ll 1$, for $\omega \in [\omega_1, \omega_2]$ is

$$\frac{B\ln\Gamma_0^{-1}}{\pi} \leq \frac{\nu_1^3}{8} + \frac{\nu_3}{2}, \tag{9}$$

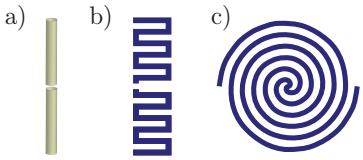

Fig. 4. Illustrations of open-circuit antennas. a) center fed dipole. b) meander line antenna. c) Archimedean spiral antenna.

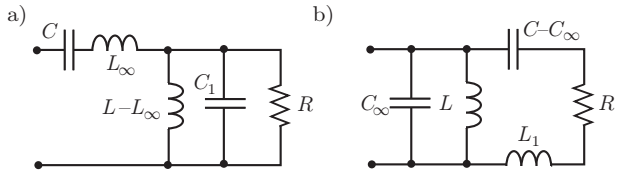

Fig. 5. Circuit representations of the resonance models. a) open-circuit (electric) antenna (16). b) short-circuit (magnetic) antenna.

where $\Gamma_0 = \max_{\omega_1 \le \omega \le \omega_2} |\Gamma(\mathrm{j}\omega)|$, $\omega_0 = (\omega_1 + \omega_2)/2$, and $B = (\omega_2 - \omega_1)/\omega_0$ denotes the fractional bandwidth. The corresponding ultra-wideband (UWB) bound on the onset angular frequency, ω_1, is

$$\omega_1 \ge \sqrt[3]{\frac{8 \ln \Gamma_0^{-1}}{\pi 3(\nu_1^3 + 4\nu_3)}}, \tag{10}$$

that is obtained with $\omega \in [\omega_1, \infty]$ and $\Gamma_0 = \max_{\omega_1 \le \omega} |\Gamma(\mathrm{j}\omega)|$, see Fig. 3b.

III. Sum rules for open-circuit antennas

The input impedance, Z, is often used to characterize antennas. It is given by a Cayley transform of the reflection coefficient and is hence a positive real function [17], [14]. Using the low-frequency expansion (3) with $\Gamma(0) = 1$ and a transmission line with the characteristic impedance Z_0, the input impedance is defined

$$\begin{aligned} Z(s) = Z_0 \frac{1+\Gamma(s)}{1-\Gamma(s)} &= \frac{2Z_0}{\nu_1 s} + sZ_0\left(\frac{\nu_1}{2} + \frac{2\nu_3}{\nu_1^2}\right) + \mathcal{O}(s^2) \\ &= \frac{1}{sC} + sL + \mathcal{O}(s^2) \quad \text{as } s \to 0, \end{aligned} \tag{11}$$

where the capacitance and inductance in the low-frequency limit are given by $C = \nu_1/2Z_0$ and $L = Z_0(\nu_1/2 + 2\nu_3/\nu_1^2)$, respectively, see also the dipole case in [22]. It is observed that the radiation resistance $R = \operatorname{Re} Z$ is $R(s) = \mathcal{O}(s^2)$ as $s \to 0$. Moreover, it is assumed that Z has the high-frequency asymptote $Z(s) = sL_\infty + \mathcal{O}(1)$ as $s \to \infty$. The high-frequency part is often unknown but it is known that positive real functions are $Z(s) = \mathcal{O}(s)$ as $s \to \infty$ in $|\arg(s)| < \pi/2$, hence the high-frequency asymptote is at most linear, see [15].

The term open-circuit antenna is used to characterize these antennas, see Fig. 4 for examples. This term is motivated by the impedance (11) that does not permit currents in the static limit. It is also seen that the series capacitance C dominates the impedance (11) for low frequencies.

The general procedure outlined in App. A states that there is one sum rule with the weight ω^2 for the radiation resistance, $R = \operatorname{Re} Z$, *i.e.*, $Z(s)/s^2$ integrated over the contour depicted in Fig. 2 gives the identity

$$\frac{2}{\pi}\int_0^\infty \frac{R(\mathrm{j}\omega)}{\omega^2}\,\mathrm{d}\omega = L - L_\infty. \tag{12}$$

This integral identity shows that the integrated radiation resistance is bounded by the low-frequency inductance. Note that $L \ge L_\infty \ge 0$ and that a lumped inductive loading increases both L and L_∞, but it does not affect R.

The corresponding admittance, $Y = 1/Z$, has the expansions

$$Y(s) = sC - s^3LC^2 + \mathcal{O}(s^4) \quad \text{as } s \to 0 \tag{13}$$

and $Y(s) = sC_\infty + \mathcal{O}(1)$ as $s \to \infty$. Here, it is observed that $C_\infty \ge 0$ and $C_\infty = 0$ if $L_\infty > 0$. The expansion (13) shows that there are at least two possible sum rules for Y. Following the procedure in App. A and integrating $Y(s)/s^2$ and $Y(s)/s^4$ over the contour in Fig. 2 gives the identities

$$\frac{2}{\pi}\int_0^\infty \frac{G(\mathrm{j}\omega)}{\omega^2}\,\mathrm{d}\omega = C - C_\infty \tag{14}$$

and

$$\frac{2}{\pi}\int_0^\infty \frac{G(\mathrm{j}\omega)}{\omega^4}\,\mathrm{d}\omega = LC^2, \tag{15}$$

where $G = \operatorname{Re} Y$ denotes the conductance. The sum rules (12), (14), and (15) are useful as they are derived under basic assumptions, and, hence, they hold for a large class of antennas.

Many antennas have a multi-resonance characteristic where it is common to utilize the first resonance. It is also observed that the weightings with ω^2 and ω^4 in (12), (14), and (15) emphasize the dynamics of the antenna around the first resonance. For these types of antennas it is interesting to compare the results with a single resonance model. Consider an antenna that is resonant at ω_0 and perfectly matched to $R_0 = Z_0$ with the input impedance having the low and high-frequency asymptotes described above. The simple resonance model

$$Z_{\mathrm{res}}(s) = \frac{1}{sC} + sL_\infty + \frac{s(L-L_\infty)}{1 + s(L-L_\infty)/R + s^2(L-L_\infty)C_1}, \tag{16}$$

based on the lumped circuit depicted in Fig. 5a can be used to model the impedance up to and around ω_0. For simplicity, the unknown high-frequency inductance is fixed as $L_\infty = 0$. The parameters R and C_1 are then given by $R = R_0 + 1/(\omega_0^2 C^2 R_0)$ and $C_1 = 1/(\omega_0^2 L) - C/(1 + \omega_0^2 R_0^2 C^2)$, respectively. The Q-factor at $\omega = \omega_0$ is easily estimated as

$$Q_{\mathrm{res}} \approx \frac{\omega_0 |Z'_{\mathrm{res}}(\mathrm{j}\omega_0)|}{2Z_0} = \frac{1}{C^2 L Z_0 \omega_0^3} + \frac{Z_0}{L\omega_0} + \mathcal{O}(\omega_0) \tag{17}$$

as $\omega_0 \to 0$, see [23], [21]. Note that the Q-factor, defined from the stored and dissipated energies in the circuit model, equals (17) with the $\mathcal{O}(\omega_0)$ term identically zero.

The sum rules for the reflection coefficient (7) and (8) with $\nu_\infty = 0$ translate into the following bounds on the fractional bandwidth, B, and the UWB onset frequency, ω_1,

$$B \le \frac{\pi C^2 L Z_0}{\ln \Gamma_0^{-1}}\omega_0^3 \quad \text{and } \omega_1 \ge \sqrt[3]{\frac{\ln \Gamma_0^{-1}}{3\pi C^2 L Z_0}}, \tag{18}$$

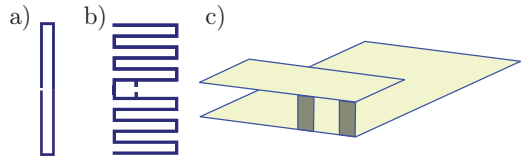

Fig. 6. Illustrations of short-circuit antennas. a) folded dipole. b) T-matched meander line antenna. c) planar inverted F antenna (PIFA).

respectively. Here, the similarities with (17) are observed, *i.e.*, $BQ_{\rm res} \leq \pi/\ln \Gamma_0^{-1}$ as $\omega_0 \to 0$ which can be compared to the case with an RCL resonance circuit [21].

IV. Sum rules for short-circuit antennas

The short-circuit antenna is formally equivalent to the open-circuit antenna with the interchange of the impedance and the admittance. Its admittance, $Y = 1/Z$, is given by

$$Y(s) = Y_0 \frac{1-\Gamma(s)}{1+\Gamma(s)} = \frac{1}{sL} + sC + \mathcal{O}(s^2) \quad \text{as } s \to 0, \quad (19)$$

where $\Gamma(0) = -1$ is used in (3), $L = \nu_1/2Y_0$, and $C = Y_0(\nu_1/2+2\nu_3/\nu_1^2)$, $Y_0 = 1/Z_0$. The corresponding impedance has the expansion

$$Z(s) = sL - s^3CL^2 + \mathcal{O}(s^4) \quad \text{as } s \to 0, \quad (20)$$

where it is observed that the radiation resistance is $R(s) = \mathcal{O}(s^4)$ as $s \to 0$ in contrast to the $\mathcal{O}(s^2)$ behavior for the open-circuit antennas in (11). The inductance and capacitance can be identified with the lumped elements of an CL parallel circuit or the resonance circuit depicted in Fig. 5b evaluated in the low-frequency limit. The expression short-circuit antenna is used to characterize these antennas, see Fig. 6 for illustrations. This is motivated by the impedance (11) that acts as a short circuit in the static limit. It is also seen that the parallel inductance L (with a magnetic field) dominates the impedance (19) for low frequencies.

The sum rules derived from (19) and (20) with the s^{-2} weight are identical to (12) and (14), however the s^{-4} case (15) is replaced with

$$\frac{2}{\pi}\int_0^\infty \frac{R(\mathrm{j}\omega)}{\omega^4}\,\mathrm{d}\omega = CL^2. \quad (21)$$

There are also corresponding relations for the reflection coefficients and bounds on the fractional bandwidth and the UWB onset frequency similar to (18).

V. A comparison with the bounds by Chu

The physical bounds by Chu are based on the Q-factor defined from the stored energy and radiated power outside a sphere with radius a that circumscribes the antenna [3], [24]. The corresponding matching bounds by Fano [8], [3], [21], [24] offer similar bounds on the fractional bandwidth, B. The bounds two show that

$$Q \geq \frac{\mathrm{c}_0^3}{\omega_0^3 a^3} + \frac{\mathrm{c}_0}{\omega_0 a} \quad \text{and } B \leq \frac{\pi\omega_0^3 a^3}{\mathrm{c}_0^3 \ln \Gamma_0^{-1}}. \quad (22)$$

for an antenna that radiates a single TE or TM mode, where c_0 denotes the speed of light of free space.

It is interesting to compare these bounds with the Q and B obtained from (17) and (18), respectively. The lowest order TM (or electrical dipole) modes have the input impedance $Z(s) = 1/sC + sL/(1+sL/R)$, where $C = \epsilon_0 a$, $L = \mu_0 a$, $R = \eta_0$, and ϵ_0, μ_0, and η_0 are the free space permittivity, permeability, and impedance, respectively [3]. Apply the estimates (17) and (18) to get

$$Q_{\rm sph} = \frac{\mathrm{c}_0^3\eta_0}{\omega_0^3 a^3 Z_0} + \frac{\mathrm{c}_0 Z_0}{\omega_0 a \eta_0} \quad \text{and } B_{\rm sph} \leq \frac{\pi\omega_0^3 a^3 Z_0}{\mathrm{c}_0^3 \eta_0 \ln \Gamma_0^{-1}}, \quad (23)$$

respectively. It is observed that the results in (23) and (22) are identical if the antenna is matched to a transmission line with the characteristic impedance $Z_0 = \eta_0$. However, many small antennas have a radiation resistance significantly smaller than η_0. A comparison with the low-frequency parameters C and L of an antenna therefore offer a new interpretation about the performance of small antennas and can be used as a tool to quantify the antenna performance in relation with the Chu bound.

The corresponding TE (magnetic dipole) modes have the input admittance $Y(s) = 1/sL + sC/(1+sC/R)$, where again $C = \epsilon_0 a$, $L = \mu_0 a$, and $R = \eta_0$.

VI. Dipole antennas

The dipole is one of the simplest open-circuit antennas. Consider a cylindrical dipole with length to diameter ratio $\ell/d = 1000$. It has its first resonance at $\omega_0 a/\mathrm{c}_0 \approx 1.5$ with the radiation resistance $R_0 \approx 73\,\Omega$, see Fig. 7 and Tab. I, where a denotes the radius of the smallest circumscribing sphere, *i.e.*, $a = \sqrt{\ell^2+d^2}/2$. The Q-factor is estimated by numerical differentiation of the impedance as in (17) to $Q_{\rm imp} \approx 8$. The numerical results are obtained from a MoM solver[1], where a gap feed model is used and the dipole is divided into 78 equidistant elements.

In Fig. 7a, it is seen that the peak around the first anti-resonance at $k_0 a \approx 2.8$ contributes substantially to the integral in (12). The contribution from the area around the first resonance is limited and hence (12) offers negligible information about the performance of the antenna in this frequency range. In contrast, the sum rules for the admittance (14) are dominated by the region around the first resonance, see Fig. 7b. The integral identity (14) for the conductance $G = \mathrm{Re}\, Y$ is hence useful in deriving bounds and estimates on the conductance for small antennas, see also the discussion in [23] on conductance bandwidth. Bound the integral in (14) over an interval $[\omega_1, \omega_2]$ as

$$G_0(\omega_2 - \omega_1) \leq \int_{\omega_1}^{\omega_2} \frac{G(\mathrm{j}\omega)}{\omega^2}\,\mathrm{d}\omega \leq \frac{\pi C}{2} \quad (24)$$

where $G_0 = \min_{\omega_1 \leq \omega \leq \omega_2} G(\mathrm{j}\omega)$. It is in general not very interesting to bound the amplitude of the conductance from below. However, if the integral (14) is dominated by the first resonance, it can be argued that the amplitude of the conductance times the bandwidth is fixed.

It is also observed that the single resonance model (16) approximates the impedance and the admittance accurately for $ka \leq 2.5$. The same is valid for the reflection coefficient $\Gamma =$

[1] www.efieldsolutions.com

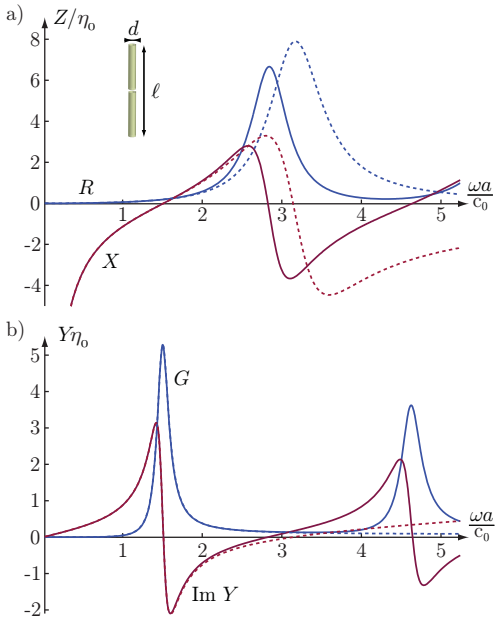

Fig. 7. a) impedance $Z = R + \mathrm{j}X$ and b) admittance Y in units of the free space impedance η_0 for the cylindrical dipole antenna with $\ell/d = 1000$. The dashed curves show the corresponding single resonance approximation (16).

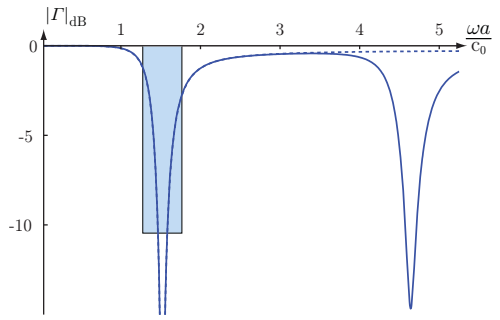

Fig. 8. The reflection coefficient $20\log_{10}|\Gamma(\mathrm{j}\omega)|$ for the cylindrical dipole antenna with $\ell/d = 1000$. The dashed curve is the corresponding single resonance approximation (16). The shaded box illustrates the bound (18).

$(Z - R_0)/(Z + R_0)$ as depicted in Fig. 8, where also a box representing the bound (18) is included.

The capacitance and inductance of the dipole can be determined with a least-squares fit of the impedance as $\omega \to 0$. However, it is also possible to determine them in the electrostatic limit by solving two additional integral equations. The low-frequency expansion of the EFIE is outlined in Appendix B and results in the two integral equations, *viz.,*

$$-\hat{\boldsymbol{n}} \times \nabla \int_{\partial\Omega} \frac{\nabla' \cdot \boldsymbol{J}_1(\boldsymbol{r}')}{4\pi|\boldsymbol{r} - \boldsymbol{r}'|}\,\mathrm{dS}' = \epsilon_0 \hat{\boldsymbol{n}} \times \boldsymbol{E}^{\mathrm{i}}(\boldsymbol{r}) \qquad (25)$$

and

$$-\hat{\boldsymbol{n}} \times \nabla \int_{\partial\Omega} \frac{\nabla' \cdot \boldsymbol{J}_3}{|\boldsymbol{r} - \boldsymbol{r}'|}\,\mathrm{dS}' - \hat{\boldsymbol{n}} \times \nabla \int_{\partial\Omega} \frac{|\boldsymbol{r} - \boldsymbol{r}'|\nabla' \cdot \boldsymbol{J}_1}{2}\,\mathrm{dS}' + \hat{\boldsymbol{n}} \times \int \frac{\boldsymbol{J}_1}{|\boldsymbol{r} - \boldsymbol{r}'|}\,\mathrm{dS}' = \boldsymbol{0}, \qquad (26)$$

where the current density is expanded in the asymptotic series $\boldsymbol{J} = s\boldsymbol{J}_1 + s^3\boldsymbol{J}_3 + \mathcal{O}(s^4)$ as $s \to 0$ and $\partial\Omega$ and $\hat{\boldsymbol{n}}$ denote the surface and unit normal of the antenna structure, respectively. These equations are solved for wire antennas, where the wire current is given by $I = \pi d \boldsymbol{J} \cdot \hat{\boldsymbol{\ell}}$. The capacitance and inductance are subsequently determined as $C = I_1(0)/V_0$ and $LC^2 = -I_3(0)/V_0$, where $I_1(0)$, $I_3(0)$, and V_0 denote the wire currents and voltage in the feed gap, respectively. Note that the asymptotic expansion is not valid for short-circuit antennas and that the integral equations (25) and (26) might have additional difficulties for surfaces that permit solenoidal currents.

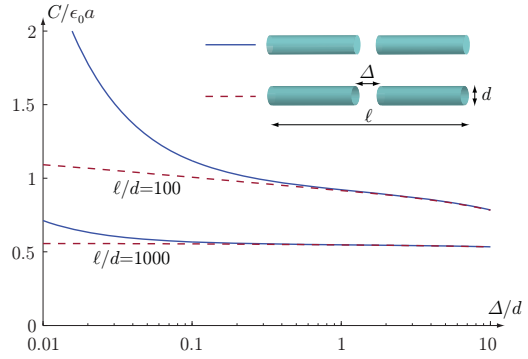

Fig. 9. Capacitance of solid (solid curves) and hollow (dashed curves) cylinders as a function of the feed distance Δ.

It is also important to realize that the capacitance in the delta gap feed model approaches infinity as the discretization approaches zero, *i.e.*, the solution with a delta gap model has a logarithmic singularity [25]. This causes the numerical solution to diverge as the resolution is refined. However, the divergence is very slow and it is common not to refine the resolution below the radius of the wire. Here, it is also essential to use the exact Green's function in the solution of the integral equation [26]. This singularity is also observed in the capacitance of the dipole, *i.e.*, the capacitance between two cylinders approach infinity as the distance, Δ, between the two cylinders deceases, see Fig. 9. Note that the capacitance of the solid cylinders approximately increases as d^2/Δ as $\Delta \to 0$ in agreement with the capacitance between two discs.

Cylindrical dipoles with semi-axis ratios $\ell/d = \{10000, 1000, 100\}$ and capacitively loaded dipoles with a length to top diameter ratio $\ell/d = \{10, 1\}$ are considered for further illustrations of open-circuit antennas, see Tab. I. The antennas are modeled with a simple delta gap in the MoM simulations. The integral equations (25) and (26) are used to determine C and L, see the table. The parameters are normalized to become dimensionless and to emphasize the similarities with the capacitance and inductance of the TM-mode, where $C = \epsilon_0 a$ and $L = \mu_0 a$, *cf.*, Sec. V. Moreover, the results are compared with the Q-factor Q_{res} obtained from the single resonance model (17). The capacitance and inductance of the dipole antennas in Tab. I are also depicted in Fig. 10, where it is observed that C increases with the thickness of the cylinder as well as with the radius of the top load for the considered antennas.

Antenna					
ℓ/d	10000	1000	100	10	1
$C/(\epsilon_0 a)$	0.39	0.55	0.96	1.07	2.7
$L/(\mu_0 a)$	0.89	0.63	0.35	0.46	0.87
$\frac{2}{\pi}\int_0^\infty R/\omega^2\,\mathrm{d}\omega/L$	0.99	0.99	0.99	1.00	1.00
$\frac{2}{\pi}\int_0^\infty G/\omega^2\,\mathrm{d}\omega/C$	0.99	0.98	0.93	0.93	0.97
$\frac{2}{\pi}\int_0^\infty G/\omega^4\,\mathrm{d}\omega/LC^2$	1.00	1.00	1.00	1.00	1.00
$\omega_0 a/\mathrm{c}_0$	1.53	1.51	1.48	1.16	0.62
R_0/η_0	0.19	0.19	0.19	0.17	0.04
$Q_{\mathrm{imp}} = \omega_0\lvert Z'\rvert/2R_0$	11	8.2	5.3	6.1	17
Q_{res}, *cf.*, (17)	11	8.0	5.0	5.9	17

TABLE I

NUMERICAL RESULTS FOR VARIOUS OPEN CIRCUIT ANTENNAS WHERE ϵ_0, μ_0, c_0, AND η_0 DENOTE THE PERMITTIVITY, PERMEABILITY, SPEED OF LIGHT, AND WAVE IMPEDANCE OF FREE SPACE, RESPECTIVELY. THE ANTENNAS ARE CIRCUMSCRIBED BY CYLINDERS WITH HEIGHT ℓ AND DIAMETER d. THE RADIUS OF THE SMALLEST CIRCUMSCRIBING SPHERE IS $a = \sqrt{\ell^2 + d^2}/2$.

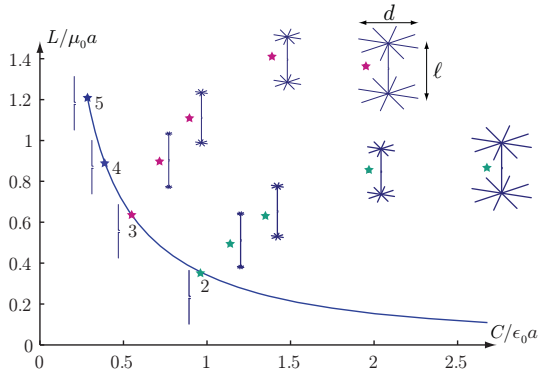

Fig. 10. The capacitance and inductance of various dipole antennas, *cf.*, Tab. I. The solid curve depicts C and L for cylindrical dipoles with $\ell/d = 10^n$, $n = 5, 4, 3, 2$ indicated by the stars on top of the curve.

VII. LOOP ANTENNA

A loop antenna is used to illustrate the sum rules for short-circuit (magnetic) antennas. The loop is modeled as a wire with radius $b = a/100$, where a is the radius of the smallest circumscribing sphere. The input impedance and admittance are depicted in Fig 11. It is seen that the first anti resonance and first resonances are at $\omega_0 a/\mathrm{c}_0 \approx 1/2$ and $\omega_0 a/\mathrm{c}_0 \approx 1$, respectively. Note that the resonance wavelength equals the circumference of the loop for $\omega_0 a/\mathrm{c}_0 = 1$. The radiation resistance is very low below the anti-resonance in agreement with the asymptote $R = \mathcal{O}(\omega^4)$ as $\omega \to 0$ in (20). The anti-resonance is very narrow and the high radiation resistance $\approx 90\eta_0$ at this frequency prohibits its use in many applications. Instead, the resonance at $\omega_0 a/\mathrm{c}_0 \approx 1$ that has a radiation resistance of $R_0 \approx 0.38\eta_0 \approx 144\,\Omega$ can be utilized in antenna applications.

The inductance and capacitance of the loop antenna are estimated to $L = 4.7\mu_0 a$ and $C = 0.87\epsilon_0 a$, respectively. It is observed that the inductance agrees well with the analytic approximation $L_{\mathrm{loop}} = \mu_0 a(\ln 8a/b - 2) \approx 4.7\mu_0 a$. The left-hand sides of the sum rules (14), (12), and (21) are

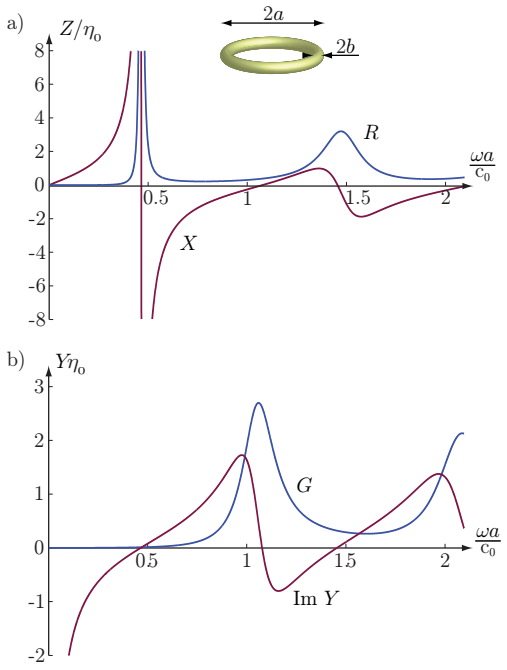

Fig. 11. a) impedance $Z = R + \mathrm{j}X$ and b) admittance $Y = 1/Z$ of a loop antenna with wire radius $b/a = 0.01$.

determined by numerical integration to $0.85C$, $0.99L$, and $1.0CL^2$, respectively. These results are in good agreement with the low-frequency parameters L and C.

VIII. CONCLUSIONS

In this paper, several sum rules valid for a large variety of antennas are introduced. The identities show that the radiation resistance (12), (21) and radiation conductance (14), (15) integrated over all frequencies are related to the low-frequency capacitance and inductance. The corresponding identities for the reflection coefficient provide bounds on the bandwidth and onset frequency expressed in the low-frequency parameters. Moreover, it is shown that the bounds are consistent with the classical bounds due to Chu [3] and that they offer additional understanding of the performance of small antennas. Although, the sum rules are most useful for small antennas that utilize their first resonance, they are valid for many electrically large antennas as well. The results are also in agreement with the approach in [4], [6], *i.e.*, physical bounds can be derived from sum rules evaluated in the low-frequency limit.

It is interesting to compare the sum rules and physical bounds presented in this paper with Fano's bounds on matching networks [8], [21], [27], [28]. The physical assumptions as well as the mathematical tools are similar. However, Fano's results provide bounds on the performance of lossless matching networks for given loads (*e.g.*, antennas). The corresponding results analyzed here relate the overall antenna performance with its low-frequency properties that in general depend on the used matching network. It should also be noted that the characterizations as open- and short-circuit antennas depend on the antenna elements as well as the feed network, *i.e.*,

matching networks can transform open-circuit antennas into short-circuit antennas and vice versa.

ACKNOWLEDGMENTS

This work was supported by the Swedish research council. The discussions with Christian Sohl and Anders Derneryd are also gratefully acknowledged.

APPENDIX

Causality, *i.e.*, the fact that the reflected signal cannot precede the incident signal, implies that $\Gamma(s)$ is holomorphic in the right complex half plane, $\operatorname{Re} s > 0$. Passivity show that $|\Gamma(\mathrm{j}\omega)| \leq 1$ for $\omega \in \mathbb{R}$ and the Phragmén-Lindelöf principle [2], [16] implies that $|\Gamma(s)| \leq 1$ for all $\operatorname{Re} s \geq 0$ since $\Gamma(s)$ does not increase exponentially, see also the discussion on passive systems in [14], [15].

Now, assume that Γ can be expanded in an asymptotic series for low-frequencies, *i.e.*, $\Gamma = \nu_0 + \nu_1 s + \nu_2 s^2 + \nu_3 s^3 + \mathcal{O}(s^4)$ as $s \to 0$, where $\mathcal{O}(s^n)$ is a term of size s^n. The coefficients ν_n, $n = 0, 1, 2, 3$ are real valued due to the symmetry requirement imposed by the time-domain origin of the reflection coefficient, *i.e.*, $\Gamma(s) = \Gamma(s^*)^*$, where the superscript * denotes the complex conjugate. The expansion coefficients are restricted by the passivity requirement $|\Gamma(s)| \leq 1$. Moreover, for a receiving antenna it is known that the accepted power of an incident plane wave with power density P_{in} is $P_{\mathrm{a}} = \sigma_{\mathrm{a}} P_{\mathrm{in}}$, where σ_{a} denotes the effective antenna aperture [29]. Now, σ_{a} equals the absorption cross section for lossless antennas and $\sigma_{\mathrm{a}} = \mathcal{O}(\omega^2)$ as $\omega \to 0$ for finite objects [30], [9]. For reciprocal lossless antennas [29], $\sigma_{\mathrm{a}} = \pi \mathrm{c}_0^2 (1 - |\Gamma(\mathrm{j}\omega)|^2) D/\omega^2$, where σ_{a} and the directivity D also depend on the direction and the polarization of the incident wave [29], [4] and c_0 is the speed of light in free space. This shows that the low-frequency asymptotic satisfy $|\Gamma|^2 = 1 + \mathcal{O}(\omega^4)$ as $\omega \to 0$ and hence $(\nu_0 - \nu_2\omega^2)^2 + \nu_1^2\omega^2 + \mathcal{O}(\omega^4) = 1 + \mathcal{O}(\omega^4)$, implying that $\nu_0 = \pm 1$. Moreover, passivity $|\Gamma(s)| \leq 1$ restricts the coefficients such that $\nu_2 = \pm \nu_1^2/2$ and $\nu_0 \nu_1 < 0$ finally giving an expansion of the form (3).

Positive real (PR) functions, $Z = Z(s)$, are defined as holomorphic mappings from the right complex half plane into itself [17]. The analogous Herglotz (or Nevanlinna) functions [2], [10] are similarly defined but in the upper complex half plane. Cauchy integrals applied to PR functions under the assumption of certain asymptotic expansions at low frequencies,

$$Z(s) = \sum_{n=0}^{N_0} a_{2n-1} s^{2n-1} + \mathcal{O}(s^{2N_0}) \quad \text{as } s \to 0 \tag{27}$$

and at high frequencies,

$$Z(s) = \sum_{n=0}^{N_\infty} b_{2n-1} s^{1-2n} + \mathcal{O}(s^{-2N_\infty}) \quad \text{as } s \to \infty \tag{28}$$

offer valuable sum rules for several electromagnetic problems. Here, the results are restricted to PR functions satisfying the symmetry $Z(s^*) = Z^*(s)$, where a star denotes the complex conjugate. Integration of $Z(s)/s^{2n}$ over the contour depicted in Fig. 2 results in the following family of integral identities:

$$\frac{2}{\pi} \int_0^\infty \frac{\operatorname{Re} Z(\mathrm{j}\omega)}{\omega^{2n}} \, \mathrm{d}\omega = (-1)^{n+1} \left(a_{2n-1} - b_{1-2n} \right), \tag{29}$$

for $1 - N_\infty \leq n \leq N_0$ and $a_n = b_n = 0$ for $n < -1$, *cf.*, [10]. Note that the integral in (29) should be interpreted as a generalized integral whenever necessary.

It is also common to use the logarithm to define PR functions from reflection coefficients. As the reflection coefficient can have zeros in the right complex half plane it is practical define a Blaschke product [2] and to factorize the reflection coefficient [8], [2]. Let s_m, $m = 1, 2, \ldots$ denote the zeros of $\Gamma(s)$ in $\operatorname{Re} s > 0$ and define the PR function

$$h(s) = -\ln \left(\Gamma(s) \prod_{m=1}^{\infty} \frac{s_m^* + s}{s_m - s} \right). \tag{30}$$

Note, that $\operatorname{Re} h(\mathrm{i}\omega) = -\ln |\Gamma(\mathrm{i}\omega)| \geq 0$ and that it is invariant under time translations, *i.e.*, multiplications with $\mathrm{e}^{s\tau}$. The low-frequency expansion of h in (30) is

$$h(s) = -\ln \Gamma(s) - 2 \sum_{m=1}^{\infty} \sum_{n=1}^{\infty} \frac{s^{2n-1}}{2n-1} \operatorname{Re} \frac{1}{s_m^{2n-1}} \tag{31}$$

as $s \to 0$.

A. Narrowband bounds

Consider the case with the $n = 1, 2$ identities in (29) for the reflection coefficient (31) that gives the inequalities

$$\frac{2}{\pi} \int_0^\infty \frac{\ln |\Gamma(\mathrm{j}\omega)|^{-1}}{\omega^2} \, \mathrm{d}\omega \leq a_1 - 2 \sum_{m=1}^{\infty} \operatorname{Re} \frac{1}{s_m} \tag{32}$$

and

$$\frac{2}{\pi} \int_0^\infty \frac{\ln |\Gamma(\mathrm{j}\omega)|^{-1}}{\omega^4} \, \mathrm{d}\omega \leq -a_3 + \frac{2}{3} \sum_{m=1}^{\infty} \operatorname{Re} \frac{1}{s_m^3}, \tag{33}$$

where $\operatorname{Re} s_m \geq 0$. This system can be solved analogous to the Fano broadband matching bounds [8], [27], [21]. Estimate the integrals in the left-hand sides, *e.g.*,

$$\begin{aligned} \int_0^\infty \frac{\ln |\Gamma(\mathrm{j}\omega)|^{-1}}{\omega^2} \, \mathrm{d}\omega &\geq \ln \Gamma_0^{-1} \int_{\omega_0(1-B/2)}^{\omega_0(1+B/2)} \frac{1}{\omega^2} \, \mathrm{d}\omega \\ &= \frac{\ln \Gamma_0^{-1} B}{\omega_0 (1 - B^2/4)} \geq \frac{\ln \Gamma_0^{-1} B}{\omega_0}, \end{aligned} \tag{34}$$

where $\Gamma_0 = \max_{|\omega - \omega_0| \leq B\omega_0/2} |\Gamma(\mathrm{j}\omega)|$ and analogous for (33). For the right-hand sides, it is observed that it is sufficient to consider a single zero s_m, *i.e.*, a sum of several zeros can always be replaced with a single zero. Set $\alpha_m + \mathrm{j}\beta_m = \omega_0/s_m$ and $\alpha_0 = \sum \alpha_m$ where $\alpha_m \geq 0$. The cubic term is

$$\operatorname{Re} \sum (\alpha_m + \mathrm{j}\beta_m)^3 = \sum \alpha_m^3 - 3\alpha_m \beta_m^2 \leq \sum \alpha_m^3 \leq \alpha_0^3, \tag{35}$$

where it is seen that the cubic term is bounded by a single zero with $\beta_0 = 0$. This simplifies the system (32) and (33)

into the system

$$\frac{B\ln\Gamma_0^{-1}}{\pi} \le \frac{a_1\omega_0}{2} - \alpha_0, \tag{36}$$

$$\frac{B\ln\Gamma_0^{-1}}{\pi} \le -\frac{a_3\omega_0^3}{2} + \frac{1}{3}\alpha_0^3. \tag{37}$$

Substitution of (36) into (37) gives

$$\frac{B\ln\Gamma_0^{-1}}{\pi} \le -\frac{a_3\omega_0^3}{2} + \frac{1}{3}\left(\frac{a_1\omega_0}{2} - \frac{B\ln\Gamma_0^{-1}}{\pi}\right)^3 \tag{38}$$

that is solved by the substitution $y = a_1\omega_0/2 - B\ln\Gamma_0^{-1}/\pi$ giving the cubic equation

$$y^3 + 3y - 3(a_3\omega_0^3 + a_1\omega_0)/2 \ge 0 \tag{39}$$

with the solution $y \ge \sqrt[3]{q+p} - \sqrt[3]{q-p}$, where $q = \sqrt{1+p^2}$ and $p = 3(a_1\omega_0 + a_3\omega_0^3)/4$. Hence the narrow-bandwidth bound is

$$\frac{B\ln\Gamma_0^{-1}}{\pi} \le \frac{a_1\omega_0}{2} - \sqrt[3]{q+p} + \sqrt[3]{q-p} \le \left(\frac{a_1^3}{24} - \frac{a_3}{2}\right)\omega_0^3. \tag{40}$$

B. UWB bounds

Consider a constant reflection coefficient over a bandwidth $\omega \ge \omega_1$, see Fig. 3. Estimate the integrals in (32) and (33) as

$$\int_0^\infty \frac{\ln|\Gamma(\mathrm{j}\omega)|^{-1}}{\omega^{2n}}\,\mathrm{d}\omega \ge \int_{\omega_1}^\infty \frac{\ln|\Gamma(\mathrm{j}\omega)|^{-1}}{\omega^{2n}}\,\mathrm{d}\omega \ge \frac{\ln\Gamma_0^{-1}}{(2n-1)\omega_1^{2n-1}}, \tag{41}$$

where $\Gamma_0 = \max_{\omega\ge\omega_1}|\Gamma(\mathrm{j}\omega)|$. It is sufficient to consider a single real-valued zero as in the narrow band case. This gives the system

$$\frac{\ln\Gamma_0^{-1}}{\pi} \le \frac{a_1\omega_1}{2} - \alpha_0, \tag{42}$$

$$\frac{\ln\Gamma_0^{-1}}{\pi} \le -\frac{3a_3\omega_1^3}{2} + \alpha_0^3. \tag{43}$$

That has the solution

$$\frac{\ln\Gamma_0^{-1}}{\pi} \le \left(\frac{a_1^3}{8} - \frac{3a_3}{2}\right)\omega_1^3 \quad \text{or } \omega_1 \ge \sqrt[3]{\frac{8\ln\Gamma_0^{-1}}{\pi(a_1^3 - 12a_3)}} \tag{44}$$

as $\omega_1 \to 0$.

The electric integral equation (EFIE) is given by [25]

$$\frac{-1}{s\epsilon_0}\hat{\boldsymbol{n}}\times\nabla\int_{\partial\Omega}\frac{\mathrm{e}^{-sR/\mathrm{c}_0}}{4\pi R}\nabla'\cdot\boldsymbol{J}(\boldsymbol{r}')\,\mathrm{dS}' + s\mu_0\hat{\boldsymbol{n}}\times\int_{\partial\Omega}\frac{\mathrm{e}^{-sR/\mathrm{c}_0}}{4\pi R}\boldsymbol{J}(\boldsymbol{r}')\,\mathrm{dS}' = \hat{\boldsymbol{n}}\times\boldsymbol{E}^{\mathrm{i}}(\boldsymbol{r}) \tag{45}$$

where $\hat{\boldsymbol{n}}$ denotes the normal unit vector and $R = |\boldsymbol{r} - \boldsymbol{r}'|$. Expand the current density in an asymptotic series

$$\boldsymbol{J} = s\boldsymbol{J}_1 + s^2\boldsymbol{J}_2 + s^3\boldsymbol{J}_3 + \mathcal{O}(s^4) \quad \text{as } s\to 0$$

and use

$$\frac{\mathrm{e}^{-sR/\mathrm{c}_0}}{R} = \frac{1}{R} - s/\mathrm{c}_0 + s^2R/2\mathrm{c}_0^2 + \mathcal{O}(s^3) \quad \text{as } s\to 0$$

This reduces the EFIE to the electrostatic integral equation (25) to the order s^0 as $s\to 0$. Solve for the normalize charge density $\rho_1 = \nabla\cdot\boldsymbol{J}_1$. The current $\boldsymbol{J}_1$ can also have an arbitrary solenoidal, *e.g.*, a constant current. Here, it is assumed that the antenna is designed such that this part vanish, hence the current $\boldsymbol{J}_1$ is uniquely determined by ρ_1.

To the order s^1

$$-\hat{\boldsymbol{n}}\times\nabla\int_{\partial\Omega}\frac{\nabla'\cdot\boldsymbol{J}_2(\boldsymbol{r}')}{|\boldsymbol{r}-\boldsymbol{r}'|}\,\mathrm{dS}' = \frac{1}{\mathrm{c}_0}\hat{\boldsymbol{n}}\times\nabla\int_{\partial\Omega}\nabla'\cdot\boldsymbol{J}_1(\boldsymbol{r}')\,\mathrm{dS} = 0$$

giving $\nabla\cdot\boldsymbol{J}_2 = 0$. Finally, (26) is obtained to the order s^2.

A delta-gap source on a wire antenna has $\boldsymbol{E}^{\mathrm{i}} = V_0\delta(\ell - \ell_0)\hat{\boldsymbol{z}}$. The current $I = I_1 s + I_3 s^3 + \mathcal{O}(s^4)$ as $s\to 0$ gives the admittance $Y = sI_1(0)/V_0 + s^3 I_3(0)/V_0 + \mathcal{O}(s^4)$. The impedance is $Z = 1/sC + sL + \mathcal{O}(s^2)$ giving $Y(s) = sC - s^3LC^2 + \mathcal{O}(s^4)$ and hence $C = I_1(0)/V_0$ and $LC^2 = -I_3(0)/V_0$.

References

[1] F. King, *Hilbert Transforms, Volume 1*. Cambridge University Press, 2009.

[2] H. M. Nussenzveig, *Causality and dispersion relations*. London: Academic Press, 1972.

[3] L. J. Chu, "Physical limitations of omni-directional antennas," *Appl. Phys.*, vol. 19, pp. 1163–1175, 1948.

[4] M. Gustafsson, C. Sohl, and G. Kristensson, "Physical limitations on antennas of arbitrary shape," *Proc. R. Soc. A*, vol. 463, pp. 2589–2607, 2007.

[5] C. Sohl and M. Gustafsson, "A priori estimates on the partial realized gain of Ultra-Wideband (UWB) antennas," *Quart. J. Mech. Appl. Math.*, vol. 61, no. 3, pp. 415–430, 2008.

[6] M. Gustafsson, C. Sohl, and G. Kristensson, "Illustrations of new physical bounds on linearly polarized antennas," *IEEE Trans. Antennas Propagat.*, vol. 57, no. 5, pp. 1319–1327, May 2009.

[7] A. Derneryd, M. Gustafsson, G. Kristensson, and C. Sohl, "Application of gain-bandwidth bounds on loaded dipoles," *IET Microwaves, Antennas & Propagation*, 2009.

[8] R. M. Fano, "Theoretical limitations on the broadband matching of arbitrary impedances," *Journal of the Franklin Institute*, vol. 249, no. 1,2, pp. 57–83 and 139–154, 1950.

[9] C. Sohl, M. Gustafsson, and G. Kristensson, "Physical limitations on broadband scattering by heterogeneous obstacles," *J. Phys. A: Math. Theor.*, vol. 40, pp. 11 165–11 182, 2007.

[10] C. Sohl, M. Gustafsson, G. Kristensson, and S. Nordebo, "A general approach for deriving bounds in electromagnetic theory," in *Proceedings of the XXIXth URSI General Assembly*, 2008.

[11] C. Brewitt-Taylor, "Limitation on the bandwidth of artificial perfect magnetic conductor surfaces," *Microwaves, Antennas & Propagation, IET*, vol. 1, no. 1, pp. 255–260, 2007.

[12] M. Gustafsson, "Sum rule for the transmission cross section of apertures in thin opaque screens," *Opt. Lett.*, vol. 34, no. 13, pp. 2003–2005, 2009.

[13] K. N. Rozanov, "Ultimate thickness to bandwidth ratio of radar absorbers," *IEEE Trans. Antennas Propagat.*, vol. 48, no. 8, pp. 1230–1234, Aug. 2000.

[14] A. H. Zemanian, *Realizability Theory for Continuous Linear Systems*. New York: Dover Publications, 1996.

[15] A. Zemanian, *Distribution theory and transform analysis: an introduction to generalized functions, with applications*. New York: Dover Publications, 1987.

[16] F. King, *Hilbert Transforms, Volume 2*. Cambridge University Press, 2009.

[17] E. A. Guillemin, *The Mathematics of Circuit Analysis*. MIT Press, 1949.

[18] T. Wu, "Some properties of impedance as a causal operator," *Journal of Mathematical Physics*, vol. 3, p. 262, 1962.

[19] M. Gustafsson and C. Sohl, "Summation rules for the antenna input impedance," in *IEEE International Symposium on Antennas and Propagation*. IEEE-AP, San Diego, July 5–12 2008.

[20] D. M. Pozar, *Microwave Engineering*. New York: John Wiley & Sons, 1998.

[21] M. Gustafsson and S. Nordebo, "Bandwidth, Q-factor, and resonance models of antennas," *Progress in Electromagnetics Research*, vol. 62, pp. 1–20, 2006.

[22] S. A. Schelkunoff and H. T. Friis, *Antennas: theory and practice*. New York: Wiley, 1952.

[23] A. D. Yaghjian and S. R. Best, "Impedance, bandwidth, and Q of antennas," *IEEE Trans. Antennas Propagat.*, vol. 53, no. 4, pp. 1298–1324, 2005.

[24] R. C. Hansen, *Electrically small, superdirective, and superconductive antennas*. New Jersey: John Wiley & Sons, 2006.

[25] J. van Bladel, *Electromagnetic Fields*, 2nd ed. Piscataway, NJ: IEEE Press, 2007.

[26] G. Fikioris and T. Wu, "On the application of numerical methods to Hallen's equation," *IEEE Transactions on Antennas and Propagation*, vol. 49, no. 3, pp. 383–392, 2001.

[27] A. Hujanen, J. Holmberg, and J. C.-E. Sten, "Bandwidth limitations of impedance matched ideal dipoles," *IEEE Trans. Antennas Propagat.*, vol. 53, no. 10, pp. 3236–3239, 2005.

[28] A. J. Mackay, "Bandwidth performance limits for finite antennas," *Microwaves, Antennas & Propagation, IET*, vol. 2, no. 5, pp. 418–426, 2008.

[29] S. Silver, *Microwave Antenna Theory and Design*, ser. Radiation Laboratory Series. New York: McGraw-Hill, 1949, vol. 12.

[30] R. E. Kleinman and T. B. A. Senior, "Rayleigh scattering," in *Low and high frequency asymptotics*, ser. Handbook on Acoustic, Electromagnetic and Elastic Wave Scattering, V. V. Varadan and V. K. Varadan, Eds. Amsterdam: Elsevier Science Publishers, 1986, vol. 2, ch. 1, pp. 1–70.